Accepted Manuscript

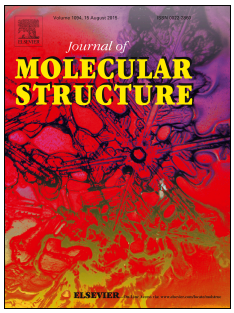

Synthesis, characterization, cytotoxicity, cell cycle analysis of 3-(4-methoxyphenyl)-1-(pyridin-2-ylmethyl)thiourea and quantum chemical analyses

Md. Mushtaque, Fernando Avecilla, Md. Shahzad Khan, Zubair Bin Hafeez, M. Moshahid A. Rezvi, Anurag Srivastava

PII: S0022-2860(17)30354-X

DOI: 10.1016/j.molstruc.2017.03.066

Reference: MOLSTR 23562

To appear in: *Journal of Molecular Structure*

Received Date: 7 August 2016

Revised Date: 15 March 2017

Accepted Date: 17 March 2017

Please cite this article as: M. Mushtaque, F. Avecilla, M.S. Khan, Z.B. Hafeez, M.M.A. Rezvi, A. Srivastava, Synthesis, characterization, cytotoxicity, cell cycle analysis of 3-(4-methoxyphenyl)-1-(pyridin-2-ylmethyl)thiourea and quantum chemical analyses, *Journal of Molecular Structure* (2017), doi: 10.1016/j.molstruc.2017.03.066.

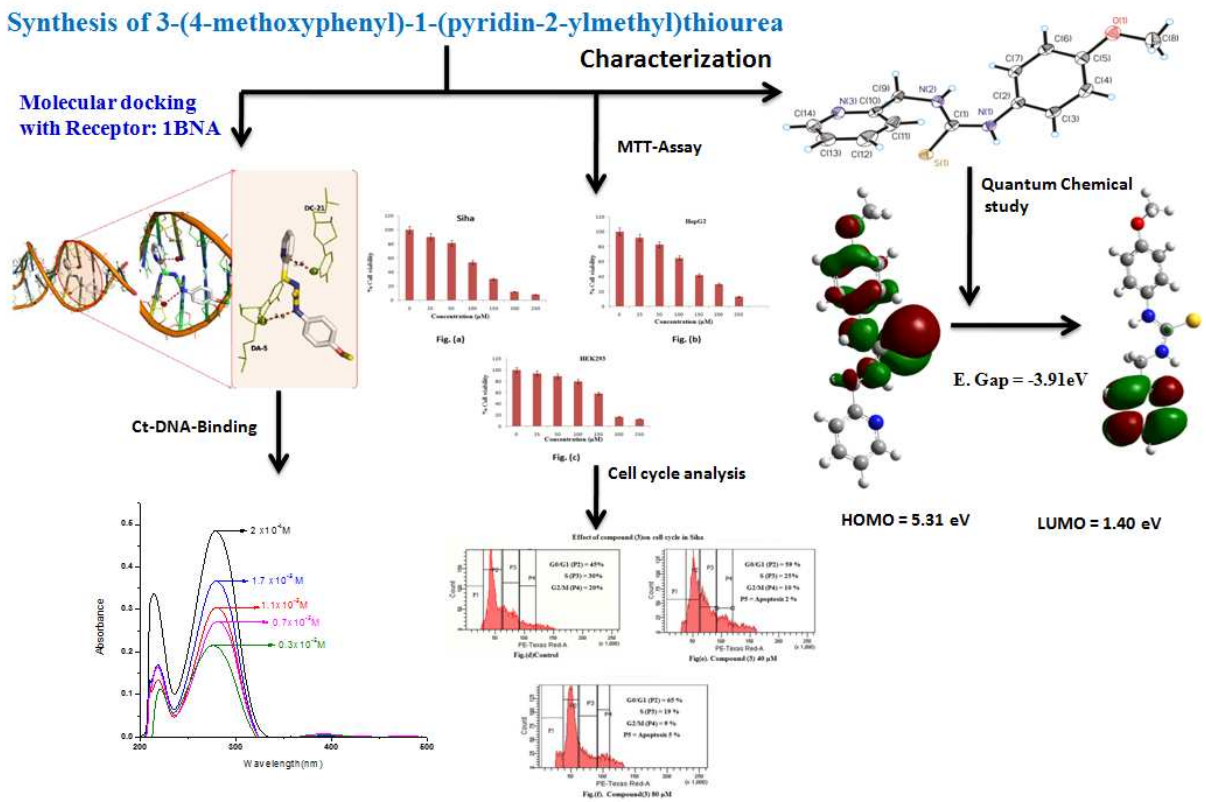

Synthesis, Characterization, Cytotoxicity, cell cycle analysis of 3-(4-methoxyphenyl)-1-(pyridin-2-ylmethyl)thioureaand Quantum chemical analyses

Md. Mushtaque[a]*, Fernando Avecilla[b], Md. Shahzad Khan[c], Zubair Bin Hafeez[d], M. Moshahid A. Rezvi[d]*, Anurag Srivastava[c]

[a]School of physical and Molecular Sciences (chemistry), Al-Falah University, Dhauj, Faridabad, Haryana, 121004, India.

[b]Departamento de Química Fundamental, Universidade da Coruña, Campus da Zapateira s/n, 15008, ACoruña, Spain.

[c]Advanced Material Research Group, CNT Lab, ABV-Indian Institute of Information Technology and Management, Gwalior 474015, India

[d]Department of Bioscience, JamiaMilliaIslamia, New Delhi, 110025, India.

Abstract: Thiourea derivative,3-(4-methoxyphenyl)-1-(pyridin-2-ylmethyl)thiourea, was synthesized. The structure of the synthesized compound **(3)** was elucidated by IR, UV-visible, ^{1}H-NMR, mass Spectrometry, and X-ray single crystal structure. The computational quantum chemical studies like, IR, UV, NBO analysis were performed by DFT with Becke-3-Lee-Yang-Parr (B3LYP) exchange-correlation functional in combination with 6-311++G(d,p) basis sets. It was observed experimentally and theoretically that compound **(3)** exhibited syn-anti-conformation around sulphur atom. The DNA-binding constant K_b was found **$3.3x\ 10^6$ $Lmol^{-1}$**. The docking energy of compound **(3)** with 1BNA was found **-6.2** Kcal/mol. MTT-assay against HepG2 (**IC_{50} = 140.39**) and Siha (**IC_{50} = 119.87 µM**) cell lines revealed that compound (3) wasnon-toxic up to**140.39 µM** against HepG2 and **119.87µM** against Siha cells respectively. It was also found that compound (3) is non-toxic against normal human cell line HEK-293(**IC_{50} = 148.67µM**). Cell cycle analyses displayed that treated HepG2 cells at 40 µM and 80 µM showed 65 % and 70 % arrest in G0/G1with respect to untreated controls (60%) and Siha cells at the same concentration displayed 59 % and 65 % arrest with respect to G0/G1 as compared to untreated control (45%).

Keywords: Cytotoxicity, Cell cycle analysis, DNA binding and molecular docking & Quantum chemical studies.

***Corresponding Author: Email: mush.chem@gmail.com**; **Contact No: +91-9891717992**

Email: rizvi_ma@yahoo.com; Contact no +91-9911661657

1. Introduction

Molecules possessing thiourea moiety are promising structural units and have great significance in modern medicinal chemistry. Thiourea is a compound composed of nitrogen and sulphur. They have been known to display various biological activities *viz*antibacterial [1], anti-fungal[2] anti-tubercular[3] anti-thyroid[4], anti-helmintic[5], rodenticidal[6] insecticidal[7], herbicidal[8], and plant growth regulator [9] activities. Thiourea derivative is one of the most promising groups of anti-cancer agents associated with a wide range of activities against various leukemia and solid tumors [10-19]. They exhibit a significant role as anti-cancer agents due to its inhibitory activity against protein tyrosine kinases (PTKs) [10-13] DNA repair synthesis [18].Recently, Camacho et.al synthesized a series of novel compounds associated with urea and thiourea of kynurenamine each with different substituents and screened against neural nitric oxide synthase (nNOS) and inducible nitric oxide synthase activity (iNOS), and he found that thiourea derivatives demonstrated the potent activity as shown in **Fig.1(a-b)**[20]. Moreover Pingaew et.al synthesized some urea and thiourea derivatives associated with 2-picolyl amine and aromatic compounds and observed that compounds(2a& 2b) exhibited potent cytotoxic effects against HepG2 and MOLT-3 cell lines as shown in **Fig2.(a-b)[21].** In the view of versatile report on different biological activities of thiourea derivatives, we here report the synthesis 3-(4-methoxyphenyl)-1-(pyridin-2-ylmethyl)thiourea derivative, and molecular docking of the compound with known receptor of DNA (PDBID:IBNA) and DNA-binding constant(Ct-DNA) by UV-Visible spectrophotometer method, and MTT-assay against HepG2, and Siha cancer cell linesand normal human(HEK-293) cell line to ensure its cytotoxic efficacy. Additionally, quantum chemical studies have also been performed in order to explore its physico-chemical properties.

2. Result and discussion

Chemistry

Compound (3), 1-(4-methoxyphenyl)-3-(pyridine-2-ylmethyl)thiourea was synthesized by reported method[22-24]as shown in **scheme(1).** The compound **(3)** was characterized by FT-IR, UV-Visible,^{1}H-NMR and mass spectrophotometer. Moreover, the structure was also confirmed by X-ray single crystal structure. The melting point was recorded 130^{0}C and is uncorrected.

The presence and absence of significant bands in the spectra confirm the formation of compound. The formation of compound (3) was confirmed by IR spectrum. The appearance of characteristic bands at 3300-3480cm^{-1} and 748 cm^{-1} were assigned to N-H and C=S bond groups which confirmed the formation of compound **(3).** In ^{1}H-NMR, chemical shift resonated at higher value the in range 9.651-9.258 ppm and 8.336-8.058 ppm as broad singlet due to presence of (-NH) and (S=CNH) protons confirmed the formation of compound **(3).**The compound (3) was also confirmed by mass spectrophotometer. The appearance of m/z; $[M+H]^{+}$ peak at 275 confirmed the formation of compounds **(3)**. Furthermore, the structure is confirmed by X-ray single crystal structure as shown in the **Fig.(3)**, and the values have been given in the experimental section.

2.1. Discussion of crystal structure

ORTEP diagram for the compound 1-(4-methoxyphenyl)-3-(pyridine-2-ylmethyl)thiourea (**3**) is showed in **Fig. (3)**.The compound (**3)** crystallizes in the monoclinic system, with $P2_1/c$ space group. The asymmetric unit of **3** only contains one molecule of the thiourea derivative. The thiourea moiety [N (2)-C1(S))-N1] form dihedral angles with the rings of the compound. A dihedral angle of 40.33(4)º with the benzene ring and of 88.34(5)º with the pyridine ring are present in the compound. The thiourea group is planar, r.m.s. deviation from plane 0.0040(5) Å. The distances corresponding to N-C and C-S bonds, in the thiourea moiety, are indicative of the Presence of amide-type resonance between the bonds N-C(=S), [N-C distances, C(1)-N(1),1.401(2) Å and C(1)-N(2), 1.354(2) Å, and C-S distance, C(1)-S(1), 1.9040(17) Å], and they are agree with the values found in literature [25]. The bond angles and bond lengths have been given in **Table (TS1)**. In the crystal packing, hydrogen atoms of the secondary amine groups participate in intermolecular interactions, with nitrogen atoms of pyridine groups and with the sulphur atoms, through the typical N–H···Shydrogen bond in this type of compounds (see **Table (TS2)** and **Fig.(4**).

3. Computational details

The ground state geometry optimizations have been carried out using DFT with Becke-3-Lee-Yang-Parr(B3LYP) exchange-correlation functional [25, 26] in combination with 6-311++G(d,p) basis sets using Gaussian09 package [27] without any symmetry constraint. To have a comparative data analysis an isolated molecule of thiourea has also been optimized with the same level of theory. The simulated IR spectrum has been analyzed using GAUSSVIEW and

VEDA 4 program to assign vibrational frequency with high degree of accuracy. The NBO and Mullikan population analysis are also reported for the local minima of title molecule. For electronic excited state calculations TD-DFT/B3LYP method has been employed with same basis set considered for ground state optimizations. The TD-DFT calculations for titled compound **(3)** are made in the background of chloroform using PCM model [28, 29].

3.1 Conformational analyses

Several thiourea derivatives displayed *syn-anti*-conformations [30-31]. In quest of stable structure and configuration, different structures of compound **(3)** have been optimized and frequencies were calculated using 6-311++G (d, p) basis sets, and the structures have been demonstrated in **Fig.5 (a-c).** From geometry optimization and frequency calculations, it was found that the configuration of structure 5(a) has local minima at potential energy surface as evidenced by no imaginary frequency. The relative energy of structure 5(a) was found-**740719.21** kcal/mol. Furthermore, the structures 5(b) and 5(c) configurations have local minima at potential energy surface as displayed no imaginary frequency. The relative energy of structure 5(b) was found-**740720.93**kcal/mol, However, relative energy of structure 5(c) was obtained -**740723.94**kacl/mol. Thus, it can be concluded that structure 5(c) has minimum energy, confirming most stable configuration, and exhibited *syn-anti*-configuration around sulphur atom. This theoretical configuration was supported by the experimental configuration as obtained by X-ray single crystal structure and was shown in **Fig.(3).**

3.2 Charge analysis

The atomic charges are reported both in terms of NBO and Mulliken's population analysis. These charges have been shown in **Table (TS3).**Qualitatively, electronic charges on constituent's atoms are same in nature for different theoretical analyses but, quantitatively, they are different. NBO analysis is fit to the chemists as it is based on localized orbital and leads to Lewis concept behavior, however, Mulliken analysis is result of canonical molecular orbital distribution which is highly delocalized and loses its significance in chemical dynamics of molecule [32]. So, further analyses have been made in terms of NBO for betterment of understanding of charge distributions. The NBO and Mulliken charges have demonstrated in the the supporting information **Table (TS3).** From the analysis, it was found that For the central part of thiourea there was a significant change in charge character of dangling sulphur atom, it has been changed from 0.07e (for isolated thiourea) to -0.286e compound(3). The N-atoms of central

thiourea region suffer electronic charge decrements from -0.86e (thiourea) to-0.6ecompound (3).Consequently, enhancement of polarity of bond length -C=S takes, resulting in the increment of its bond length.

3.3 IR analysis

The 1-(4-methoxyphenyl)-3-(pyridine-2-ylmethyl)thiourea consists of 34 atoms which consequences to 96 normal modes of fundamental vibrations. This molecule belongs to C1symmetry. Up to the best of our knowledge none have reported the quantum chemical study for molecular structure and IR-spectrum of 1-(4-methoxyphenyl)-3-(pyridine-2-ylmethyl) thiourea.The observed and calculated IR-spectra have been presented in **Fig. 6(a-b)**.The rigorous analysis for fundamental modes of vibration with B3LYP has been demonstrated in **Table (TS4)** and Veda 4 Programme[33-36] has been used to assign to vibrational frequency. In our study we have scaled B3LYPcalculation with 0.98 to correct the theoretical error[37].

C-H vibrations

The theoretical C-H stretching modes of vibration of compound (3) were calculated in the range of 3000-3229cm^{-1}. The C-H terminal of methyl group displayed asymmetric vibration at 3058 cm^{-1} and symmetric vibration at 3000 cm^{-1} theoretically, however, its experimental counterpart were observed at 3000 cm^{-1} and 2931 cm^{-1}. Theoretical C-H vibrations associated with benzene were found at 3229 cm^{-1}, 3202 cm^{-1}, 3195 cm^{-1} and 3157 cm^{-1} with more than 88% contributions. C-H vibrational peak associated pyridine was majorly found at 3184 cm^{-1}, 3168 cm^{-1} and 3163 cm^{-1}. The in-plane bending vibrations of H-C-C was calculated in the region of 1129-1660 cm^{-1} and particularly, wave numbers were 1129 cm^{-1}, 1135 cm^{-1}, 1171 cm^{-1}, 1175 cm^{-1}, 1194 cm^{-1},1250 cm^{-1} and 1467 cm^{-1}, 1478 cm^{-1}, 1491 cm^{-1}, 1637 cm^{-1} and 1660 cm^{-1}. The plane torsional bending of H-C-C-C was at 751 cm^{-1}, 840 cm^{-1}, 949 cm^{-1}, 953 cm^{-1} and 1014 cm^{-1}. Calculated wave number at 1478 cm^{-1} was assigned to bending vibration of H-C-H which was of methoxy group, however, its experimental value was found at1464 cm^{-1}. Other modes of vibration have been given in **Table (TS4).**

O-C vibrations

The theoretical ethereal (-O-C) wave numbers of methoxy group were observed at 1506 cm^{-1}, 1491 cm^{-1}, 1065 cm^{-1}, 1171 cm^{-1}, and 521 cm^{-1}. But its experimental values were observed at 1498 cm^{-1}, 1171 cm^{-1}, 841 cm^{-1} and544 cm^{-1}. The bending vibration of C-O associated with C15-O18-C19 was observed at 533 cm^{-1}.The torsion associated with H33-C19-O18-C15 of C-O with

57% contributions was observed at1171.0 cm^{-1}. The stretching vibration of C-O associated with O18-C19 with 75 % contribution was found at 1065 cm^{-1}. The wave numbers associated with H32-C19-O18-C15, H34-C19-O18-C15 and H33-C19- O18-C15 at 1506 cm^{-1} and 1491$cm^{-1}$of C-O were found torsional in nature.

N-H vibrations

Normally, N-H stretching vibrations are observed in the region of 3500-3200cm^{-1}. The band observed at 3481 cm^{-1} in FT-IR spectrum was assigned to N-H and its theoretical values were assigned at 3602 $cm^{-1}$and 3563cm^{-1}. The rest of vibrations associated with nitrogen have been displayed given in **Table [TS4].** Saeed et.al [38] reported for free -NH_2 group, symmetric and asymmetric stretching were observed at 3324 cm^{-1} and 3114cm^{-1} respectively. Lower value of symmetric stretching was due to intramolecular hydrogen bonding. However, in our reported compound (3), -NH stretching was observed at 3481 cm^{-1}.Saeed et.al also reported the intense peak of -NH deformation at 1619 cm^{-1} and 1547 cm^{-1}. But inour case, NH deformation was observed at 1593 cm^{-1}.

C-N vibrations

The stretching vibrations and including other vibration modes of C-N were found in the range of 1062-1407cm^{-1}. However, the most effective wave numbers associated with C-N were observed at 982 cm^{-1}, 1014 cm^{-1}, 1067 cm^{-1}, 1296 cm^{-1} and 1637 cm^{-1}. The out of plane mode of vibration of CN associated with C7-C6-N4-C5 was calculated at478 cm^{-1}. Rest modes have been given in **Table (TS4).**

C=S vibrations

The experimental stretching vibration of C=S of compound (3) was at 758 cm^{-1}, however, its theoretical values was found at 748 cm^{-1}.

3.4 NBO analysis

NBO analysis depicts the role of inter and intramolecular bonding. It is suitable to find charge transfer or hyper conjugative interactions in molecular systems. The energy of interacting orbital differences is proportional to the stabilization of orbital interactions. Thus, the prominant interactions of stabilization occur between dominant donors (i) and acceptors (j). Quantatively, the interactions between bonding anti-bonding orbitals are interpreted in terms of NBO basis, and is expressed by means of second order perturbation interaction energy, E(2)[39]. This energy

describes an estimate of off diagonal NBO Fock matrix element. The stabilization energy is calculated by following mathematical expression.

$$\mathbf{E2=\Delta Ei,j=qi\frac{F(i,j)2}{\varepsilon i-\varepsilon j}} \quad \mathbf{(1)}$$

Where qi is donor orbital occupancy, εi and εj are diagonal elements (orbital energy) and F(i, j) Is off diagonal Fock matrix. In our studied compound, Second lone pair electron of S11 is strongly disperses into anti-bonding orbital σ*(N8-C9) and σ* (C9-N10) through hyperconjugation, resulting hyperconjugative stabilization energy 10 and 13 Kcal/mol. Lone pair of electron of oxygen resonated to anti-bonding molecular orbital π*(C14-C15) and gave stabilization energy 30 Kcal/mol. Furthermore, Lone pair electrons from N8 and N10 are strongly interacted to π-anti-bonding orbital of C9-S11 but the electronic charge and hence C9-S11 loses its double bond character which is also evident in terms of its bond length value of1.35Å instead of 1.37Å for pristine thiourea. The stabilization energy for such hyper conjugation is 77 and 68kcal/mol. However, F. Weinhold reported that lone pair of electron of nitrogen of formamide showed strong hyperconjugation to anti-bonding orbital of π*(N-CO) which led to conjugative stabilization 60 Kcal/mol[40] which is less than our title compound. It was also reported that the nitrogen around thiocarbamate, urea and thioester occupied planar structures[41-42] which are important for the strong resonance and exhibiting conjugative stabilization energy. Saeed et. al found conjugative energy of urea and thiocarbamate 56 and 41 kcal/mol,due to the intreraction of lone pair of nitrogen to the anti-bonding orbital of π*(CO [43] and are not greater than our studied compound. Furthermore, lone pair of electron present on nitrogen of pyridine dispersed into anti-bonding molecular π*(C5-C6) through intramolecular charge transfer, causing stabilization energy 10 Kcal/mol. However, Saeed et. al found [44] that lone pair of electron on nitrogen interacted with anti-bonding **π*** (C=C) orbital through resonance and conjugative stabilization energy was observed to 35 Kcal/mol which is almost three times higher than our title compound. Additionally, The bonding molecular orbital of π (C14-C15) interacted with anti-bonding molecular π*(C12-C13) through intramolecular charge transfer and gives stabilization energy 22 Kcal/ mol. The stabilization energy has been given in **Table (TS5).**

3.5 UV-Visible analysis

In order to describe the nature of electronic transitions within 1-(4-methoxyphenyl)-3-(pyridine-2-ylmethyl)thiourea, TD-DFT calculation was performed in chloroform solvent background. The

theoretical wavelength was obtained from UV-Visible spectra with B3LYP/6-311G++(d,p) level of theory for twelve lowest singlet state. The experimental and theoretical electronic spectra are shown in **Fig.7(a-b)**. The comparative theoretical and experimental electronic transitions are given in **Table (TS6).** The inter-frontier orbitals obtained from TDFFT calculations at the contour value of 0.02, as shown in **Fig.(8),** are used to analyze the nature of electronic transitions. The first theoretical electronic transition was obtained at 276 nm wavelength (λ_{max}). However, its experimental wavelength was observed at 278 nm. This transition is majorly contributed from HOMO-1 to LUMO+3 which is primarily n→π* in nature. This transition takes place from bonding orbital of suphur to anti-bonding orbital of 4-methyl benzyl ring as evidenced from **Fig.(8).** The second theoretical electronic transition was observed at 236 nm wavelength (λ_{max}) and experimental transition was found at 214 nm. This transition involves HOMO to LUMO+4 and LUMO+5 molecular orbitals. The nature of transition is π→π* in nature. The transition takes place from π-bonding orbitals of 4-methyoxy benzyl group to anti-bonding orbitals of the same group and pyridine ring as is cleared from the **Fig.(8)**.

3.6 Frontier Molecular Orbital

In order to know the physico-chemical behavior and energy associated with compound(3), HOMO and LUMO energy and energy gap are calculated using optimized geometry with B3LYP/6-311++G(d,p) basis set and is represented in **Fig.(9).** The positive and negative phases of the molecular orbitals have been shown in red and green color respectively. The chemical reactivity and biological efficacy depend upon the eigen value of HOMO and LUMO energy and energy gap [45]. The molecule possessing smaller interfrontier orbitals are chemically more active and have lower kinetic stability [23-24]. Moreover, the electrical and optical properties and electronic transition and chemical reactions are described by HOMO and LUMO molecular orbitals[46,47]. They also signify the electron donating and accepting abilities. They are also helpful in interpreting the electronic transition from ground state to first excited state [45]. From **Fig.(9),** it can be observed that HOMO molecular orbital is comprised of C(17, 14, 13) and C(12, 15 & 16), N(10), C(9), S(11) and N(8) and LUMO molecular orbital is spread over pyridine ring. HOMO-1 orbital is spread over thiourea part of compound (3). However, HOMO-2 is spread over entire molecule except pyridine ring. But HOMO-1 and HOMO-2 participate in electronic transition as shown in **Fig.(8).**

Some new chemical descriptors have been proposed *viz* ionization energy (**I.E**), electron affinity (**E.A**), electronegativity(***χ***), chemical potential(***μ***), global harness(***η***), softness(**s**) and global electrophilicity index(**ω)** to understand the various aspects associated with pharmacological sciences, drug design and possible eco-toxicological features of the drugs. All these are calculated using HOMO and LUMO energy. The structure and reactivity of a compound can also be understood by them. The mathematical expression and calculation of the studied compound **(3)** are given in **Table (1).** From the calculation, the ionization energy and electron affinity were found **5.31 eV and 1.40 eV**. However, the chemical potential, electronegativity, softness and global electrophilicity index were found **-3.35eV, 3.35eV, 0.26eV^{-1} and 2.88eV** respectively. The energy gap between HOMO and LUMO was found **3.91 eV.** This energy gap explains the charge transfer interactions with the molecule, and affects biological activity of the compound. The concept of global electrophilicity index was proposed by Parr et al[48] and is used to calculate the stabilization energy when an extra electronic charge is transferred to the molecular system from environment. It also explains the ability of an electron to gain additional electronic charge and resistance of the molecule to exchange the electronic charge with surroundings. The chemical potential and hardness are useful for global chemical reactivity. The chemical potential of compound **(3)** is negative which clearly indicates that compound is stable and can not decompose spontaneously. Hardness offers resistance to the molecule so that electron cloud could not deformed under the influence of perturbations encountered during the chemical reactions. Larger the energy gap between HOMO and LUMO, greater would be the hardness and would be more stable and less reactive and is less polarizable and vice-versa.

Aswathy et.al reported 1-(3,4-dichlorophenyl)-3-[3-(trifluoromethyl)phenyl]thiourea derivative[49]. He found that the chemical potential of the reported compound was **-5.934 eV.** On the other, War et.al also reported 1-[3-(1H-imidazol-1-yl)propyl]-3-phenylthiourea derivative and it was found that chemical potential of compound was **-3.3475 eV** [50]. Furthermore, in our previously reported compound, 1-(4-methoxyphenyl)-3-(pyridine-3-ylmethyl)thiourea derivative, chemical potential was reported **-3.37 eV** [23]. But in our studied compound (3), chemical potential is **-3.35 eV**. As we know that higher the negative chemical potential, greater is the reactivity. On the on the basis of this fact, order of reactivity can be compared. Thus, studied compound (3) is less reactive than 1-(3, 4-dichlorophenyl)-3-[3-(trifluoromethyl)phenyl]thiourea

derivative and our previous reported compound1-(4-methoxyphenyl)-3-(pyridine-3-ylmethyl)thiourea. However, the reactivity of compound (3) is comparable with 1-[3-(1H-imidazol-1-yl)propyl]-3-phenylthiourea derivative.

4. Pharmacology

DNA-binding

Nowadays, DNA has become widely used target for a large number of pharmaceutical active and anti-cancer compounds. Many organic metal complexes and organic compounds are known to bind with DNA in a various ways [51-52]. So, the study of interactions with new compounds with DNA is a crucial step for developing new drugs. In this context, UV–visible spectroscopy is one of the most commonly working techniques [53]. Through, UV-Visible spectrophotometric titration, hypochromic and hyperchromic shifts with change in wavelength, absence or presence of isosbestic points are observed, which are the characteristics of interactions of compounds with DNA[54-55]. Classically, hypochromism and bathochromism display a non-covalent binding, however, hyperchromism shows covalent binding[53]. In our experiment, the significant peak appeared in the range of 200-420 nm showed the interactions of a compound (3) with ct-DNA and has been demonstrated in **Fig. 10(a&b)**. It was also observed that the second band was shifted slightly, and it was because of intra ligand $\pi \rightarrow \pi^*$ transitions [54, 56]. The presence of band at the range of 218-250 nm indicated that there was $\pi \rightarrow \pi^*$ transition. The second band appeared at 250-350 nm which exhibited $n \rightarrow \pi^*$ transition. These experimental data suggested the bathochromic shift, due to interactions of compound (3) with DNA. It was also observed that with the addition of different concentrations of DNA [0.45-3.8x 10^{-5} M], the absorption peaks underwent hypochromicities for the target compound **(3),** thus, pointing out the formation of DNA-compound adducts [57]. Furthermore, the binding constant of compound**(3)** was found to be(K_b) **$3.3x10^6$ $Lmol^{-1}$**which is in good agreement with molecular docking.

4.2 ***Cell cycle perturbation***

Result & discussion

To insure the effects of compound **(3)** on cell cycle perturbation, the flow cytometry assay technique was performed against HepG2 and Siha cell lines. In present work, treated HepG2 cells at concentration ranges 40μM and 80 μM exhibited the cell cycle phase distribution 65%and 70% respectively arrest in G0/G1 as compared to untreated control (60%) as shown in **Fig. 11 (a-c).** However, at concentrations 40 μM, and 80 μM, treated Siha cells displayed cell

cycle distribution 59% and65 % respectively arrest in G0/G1 as compared to untreated control (45%) as in **Fig.11 (d-f).** Thus, it can be concluded from data that compound **(3)** induced the cell cycle arrest G0/G1 in both HepG2 and Siha cell lines.

4.3 MTT Assay

3-(4,5-dimethylthiazol-2-yl)-2,5-diphenyl tetrazolium bromide (MTT) is an important dye reduced by succinate dehydrogenase enzyme of mitochondrial living cells to produce water insoluble purple formazan crystals[58-59]. MTT assay has widely been used to find the cytotoxic effects of the synthetic /Natural compounds/Extract[60-61]. The cytotoxicity of compound **(3)** was performed against HepG2, Siha and HEK-293 cells for 48 hours treatment at concentration range 0-250 μM as shown in **Fig.12(a-c)**. In the present study, it was observed that compound **(3)** displayed non-cytotoxic effect against both the concerous cell lines, HepG2 (IC_{50}= 140.39 μM) and Siha (IC_{50}= 119.87μM). Compound **(3)** was also found non-cytotoxic against HEK-293(IC_{50} = 148.67μM). Hence, compound **(3)** was non-cytotoxic againstHepG2 Cells and Siha cells at the concentration ranges 0-140 μM and 0-120 μM respectively, and also non-toxic against HEK-293 up to the concentration range 0-149 μM.

4.4Molecular docking

Virtual screening and computational study has become most commonly used tool for drug development [62]. This may be fast outcomes of prediction of binding sites, low expenses and free availability of much software [63]. In order to examine, our experimental results, DNA docking study has been carried out through Auto Dock-Vinal tool [64-65]. The docking study of the compound (3) was performed with DNA dodecamersd(CGCGAATTCGCG)2 (PDB ID: 1BNA). The binding energy of the docked compound **(3)** was found to be **-6.2 Kcal/mol**. It was observed that molecule preferred to interact with base pair of DNA as shown in **Fig. (13),** and made polar and several no-polar interactions and displayed in **Fig.(FS1),** and data have been presented in **Table (TS7**). This molecular orientation of compound **(3)** confirmed formation of two H-bonds hydrogen bonds with chain B (**B: DC'21/O2::N** of thiourea **(0.244)** and chain A(**A: DA'5/O4:: N** of pyridine **(0.356)**. Thus, docking study supported our experimental results.

4.5 Mechanism of action at supramolecular level

UV-visible spectroscopic data, it was observed that compound **(3)** formed adducts with DNA due to covalent and non-covalent bindings. The docking studies also suggested that compound **(3)** bound with DNA bases and a compound **(3)** behaved as intercalating agent. The intense

evaluation and 3-D visualization of compound **(3)** showed that 4-Methoxy-substituted phenyl ring and pyridine rings were present in between the chains A and B as shown in **Fig. (13)** Nitrogen of pyridine formed one hydrogen bond with **Guanine-cytosine** base pair of DNA, and however**,** nitrogen of thiourea associated with 4-methoxy benzene formed hydrogen bondwith **Adenine-thymine** base pairs of DNA as depicted in **Table (TS7).** It can be said that the major force for the interactions of compound **(3)** with DNA is hydrogen bonding. Steric effects and Vander Waal's force also played vital role in binding of compound **(3)** with DNA. Thus, compound **(3)** has an affinity towards DNA, which is in accordance with the experimental UV–visible spectroscopic data [23].

5. Conclusion

From our experimental results, it can be concluded that compound **(3)** adopted *syn-anti*-conformation. The ionization and electron affinity were found to be **5.31eV** and **1.40eV.**The DNA-binding constant was found **3.3 x 10^6** $Lmol^{-1}$. Compound **(3)** displayed binding energy **-6.2** Kcal/mol. Cell cycle phase distribution demonstrated that treated HepG2 cells showed 65 % and 70% arrest in G0/G1in comparison with untreated control (60%). However, Siha cells, displayed 59 % and 65 % arrest in G0/G1 as compared to untreated control (45%). From MTT-assay, it was found that compound (3) displayed non-cyctotoxic nature against cancerous cell lines, HeG2 (IC_{50} = 140 μM), and Siha(IC_{50} = 119.67 μM), and also normal human cell lines HEK-293(IC_{50} = 148.87 μM). Hence, compound **(3)** was toxic at concentrations greater than 140 μM against HepG2 cells and against Siha at 120 μM.

6. Experimental protocol: All the required chemicals were purchased from Merck and Aldrich Chemical Company (USA). Precoated aluminium sheets (Silica gel 60 F254, Merck Germany) were used for thin-layer chromatography (TLC) and spots were visualized under UV-light. FT-IR spectra were recorded on Perkin Elmer model 1600 FT-IR RX1 spectrophotometer as KBr discs.^{1}H-NMR and ^{13}C-NMR spectra were recorded on Bruker Spectrospin DPX 300 MHz using $CDCl_3$ as a solvent and trimethylsilane (TMS) as an internal standard. Splitting patterns are designated as follows; s,singlet; d, doublet; m, multiplet. Chemical shift values have been given in ppm. The ESI-MS was recorded on micrOTOF-Q II 10330 Electronspray ionization mass spectrometer (Bruker). X-ray data were collected on Bruker SMART Apex CCD diffractometer (SAI, Universidade daCoruña).

6.1 Synthesis of thiourea derivative

one mole of picolylamine was taken in 10 ml of toluene in round bottom flask. To it, 1 mole of 4-methoxy phenylisothiocynate was slowly added and reaction mixture was stirred at room temperature. The Progress of reaction was monitored by TLC (5% Chloroform and Methanol). Solid white product was obtained with 30 minutes. The product was filtered and washed with toluene and recrystallized in chloroform which yielded light white crystalline solid.

6.1.1 1-(4-methoxyphenyl)-3-(pyridine-2-ylmethyl)thiourea (m.p. 130 ^{0}C): (Yield: 90 %): IR (λmax) cm^{-1}; 3467.14(-NH-Ar), 3341.80(-NH-), 3147.68 (Ar-H), 2989.67(OCH_3), 1519.67(CN),1242.69(C=S), ^{1}H-NMR(DMSO-d6):9.651(bs, 1H, NH-Ar), 8.058(bs, 1H, -NH-C=S), 8.511(d,1H, J = 3.3 Hz, Ar-H), 7.792(t, 1H, J = 7.5 Hz, Ar-H), 7.339-7.257(m, 4H, Ar-H), 6.932 (d, 2H, J= 6.6 Hz, Ar-H), 4.799 (d, 2H, J = 5.4 Hz, CH2N-), 3.745(s, 3H, OCH3); m/z;[M+H]+= 275

6.2 X-Ray crystal structure determination

Three-dimensional X-ray data were collected on a Bruker Kappa Apex CCD diffractometer at low temperature for **3** by the ϕ-ωscan method. Reflections were measured from a hemisphere of data collected from frames, each of them covering 0.3º in ω. A total of 28849 reflections measured were corrected for Lorentz and polarization effects and for absorption by multi-scan methods based on symmetry-equivalent and repeated reflections. Of the total, 2314 independent reflections exceeded the significance level ($|F|/\sigma|F|$) > 4.0. After data collection, in each case an multi-scan absorption correction (SADABS)[66] was applied, and the structure was solved by direct methods and refined by full matrix least-squares on F^2 data using SHELX suite of programs[67]. Hydrogen atoms were located in difference Fourier map and left to refine freely, except for C(8), were included in calculation position and refined in the riding mode. A final difference Fourier map showed no residual density in the crystal 0.371 and -0.231 e.Å^{-3}. A weighting scheme w = $1/[\sigma^2(F_o^2) + (0.054100\ P)^2 + 0.515500\ P]$ was used in the latter stages of refinement. Further details of the crystal structure determination are given in **Table (2).** CCDC 1448611 contains the supplementary crystallographic data for the structure reported in this paper. These data can be obtained free of charge via http://www.ccdc.cam.ac.uk/conts/retrieving.html, or from the Cambridge Crystallographic Data Centre, 12 Union Road, Cambridge CB2 1EZ, UK; fax: (+44) 1223 336 033; or e-mail: deposit@ccdc.cam.ac.uk. Supplementary data associated with this article can be found, in the online version, at doi: $$$$$.

6.3 Cytotoxicity studies (MTT assay)

Cell culture

Human hepatocellular carcinoma cell line (HepG2), Cervical cancer cell line (Siha, Hela), Breast cancer cell (MCF-7) and Human Embryonic Kidney cell line (HEK-293) were procured from National Curator of Cell Sciences (NCCS) Pune, India. Cells were cultured in Dulbecco'smodified Eagle's medium (DMEM) with 10 % fetal bovine serum with 100 units/mL penicillin, 100 µg/mL streptomycin, and 2.5 µg/mL amphotericin B, at 37 0C in a relative humidity 80 % , 5% CO2[68].

MTT assay

Cytotoxicity of compound (3) was evaluated through MTT (3-(4,5-dimethylthiazole-2-yl)-2,5-diphenyl tetrazolium bromide, M2128 Sigma Aldrich) assay onHepG2, Siha, and HEK-293 cells. MTT is a validated assay for the *in vitro* cytotoxicity of any natural, synthetic compounds and extracts [69-70]. The cell count $1.2x10^4$ cells/well was seeded in 96 well plate (150 µL/well). After overnight incubation, cells were treated with different concentrations of compound (3) for 48 hours. After 48 hours treatment, medium was removed and incubated with 20 µL of MTT solution (5 mg/mL in Phosphate saline buffer) for 4 hours. The formazan crystals were formed by mitochondrial enzyme reduction, finally solublized in DMSO (150 µL/ well) and absorbance was recorded at 570 nm through the Microplate reader (iMark, BIORAD, S/N 10321). Percent viability was defined as the relative absorbance of treated versus untreated control cells.

6.4DNA-binding

The stock solution of disodium salt of Ct-DNA was prepared in tris-HCl buffer (pH 7.2–7.3) and stored at 4^0C temperature. Once prepared, the stock solution was used within 4 days. The concentration of the solution was determined spectrometrically. The ratio of absorbance at 260 and 280 (≥1.8) indicated that DNA was sufficiently free of protein. The concentration of DNA was measured using its extinction coefficient at 260 nm (6600 M^{-1} $cm^{-1)}$ after dilutions. For the titration purpose, DNA stock solution was diluted using tris-HCl buffer. The compound **(3)** was dissolved in minimum amount of DMSO (2.0×10^{-4} M). UV-visible absorption spectra were recorded after each addition of different concentrations of DNA. Absorption titration was conducted by adding varying concentrations ($0.3\text{-}1.7 \times 10^{-5}$ M) of DNA. The intrinsic binding constant (K_b)was determined by Eq. (1), which was originally known as Benessi–Hilderbrand equation and further modified by Wolfe et al[71].

$$\mathbf{[DNA]/(\varepsilon_a - \varepsilon_f) = [DNA]/(\varepsilon_a - \varepsilon_f) + 1/Kb\ (\varepsilon_b - \varepsilon_f)} \quad (1)$$

Where the apparent absorption coefficients ε_a, ε_f and ε_a correspond to A obs/[compounds], the extinction coefficient for compound**(3),** and the extinction coefficient for compound **(3)** in the fully bound form. In plots of [DNA]/(εa− εf) versus [DNA], Kb is given in the ratio of the slope to intercept.

6.5 DNA docking studies

Docking studies were performed at Intel(R) Core(TM) i3 CPU (2.3 GHz) with XP-based operating system (Windows 2007). 3D Structure of compound **(3)** was drawn by Mercury software using CIF file of crystal structure and saved in pdb file format. The preparation of the compounds was done by assigning Gastegier charges, merging non-polar hydrogens, and saving it in PDBQTfile format using AutoDock Tools (ADT)4.2 [64-65]. The X-ray crystal structure of DNA (PDB ID:1BNA) was obtained from the Protein Data Bank [Protein Data Bank. Available online at:http://www.rcsb.org/pdb]. Using ADT 4.2, DNA was saved in PDB file format leaving heteroatoms(water). Gastegier charges were assigned to DNA and saved in PDBQT file format using ADT. Preparation of parameter files for grid and docking were done using ADT. Docking was performedwith Auto-Dock4.2 (Scripps Research Institute, USA), considering all the rotatable bonds of ligandas rotatable and receptor as rigid[72] Grid box size of **80 × 80 × 60** Å with **0.375** Å spacing was usedthat included whole DNA. In the present work, we describe a plug in for PyMOL which allow scarrying out molecular docking, virtual screening and binding site analysis with PyMOL. The plug inrepresents an interface between PyMOL and two popular docking programs, Autodock [64-65], AutodockVina [74] and also the extensive use of a Python script collection (Autodock Tools) [73].

6.6 Methodology of Cell cycle analysis

Flow cytometry was performed for analysis of cell cycle arrest according to the standard method[74]. The effects of compound **(3)** on cell cycle on Siha and HepG2 cell lines were analyzed by flow cytometry. After reaching 70% confluency, cells were serum starved overnight and treated with compound **(3)** for 48 h in complete medium. The cells were trypsinised, washed two times with chilled PBS and centrifuged at 1500 rpm for 5 minutes. Further, 1ml chilled 70% ethanol was added drop wise to the cell pellet and vortexed gently. The cells were incubated for 1 h at 4ºC. The cells were centrifuged at 2000 rpm for 5 minutes, and the pellet was washed twice with PBS. The cells were re-suspended in 500 µl PBS, added 10µl ribonuclease(100µg/ml final concentration) and incubated for30 min at 370C. Cells were stained with propidium iodide

(50 μg/ml final concentrations) and incubated for 15 min. Flow cytometry analysis was performed with FACS (Becton Dickinson). A minimum of 10,000 cells were acquired. Further, histogram was analyzed by Flowjo software for cell cycle analysis.

Acknowledgment

One of the authors, **Md. Mushtaque,** is highly thankful Science and Engineering Research Board (SERB) Govt. of India, for financial assistance, and **Professor Stephen Husbands** (Department of Pharmacy and Pharmacology, University of Bath, Claverton Down, BA2 7YA, U.K.) and chancellor (**Mr. Jawad Ahmed Siddiqui**) of Al-Falah University.

References

1. M. K. Mallath, D. G Taylor, R. A. Badwe, G. K. Rath, V. Shanta, C. S. Pramesh, R.Digumarti, P. Sebastian, B.B. Borthakur, A. Kalwar, S. Kapoor, S. Kumar, J. L.Gill, M. A.Kuriakose, H. Malhotra, S.C. Sharma, S. Shukla, L. Viswanath, R. T. Chacko, J. L. Pautu,K.S. Reddy, K.S. Sharma, A. D. Purushotham, R. Sullivan. Lancet Oncol.15(2014) e205–212.
2. F. Bray. B. Moller, Nat. Rev. Cancer**.** 6 (2006) 63–74.
3. L.A.Shervington, N. Smith, E. Norman. T. Ward, R. Phillips, A. Shervington, Eur. J. Med. Chem. 44 (2009) 2944–2951.
4. K. Loven, L. Stein, K. Furst, S. Levy, ClinTher.24 (2002) 990–1000.
5. A. Skladanowski, J. Konopa. BiochemPharmacol.46 (1993) 375–382.
6. R. Lesyk, B. Zimenkovsky, Curr. Org. Chem.8 (2004) 1547–1577.
7. R. Lesyk, O. Vladzimirska, S. Holota, L. Zaprutko, A. Gzella, Eur. J. Med. Chem. 42(2007)641–648.
8. D. Havrylyuk, B. Zimenkovsky, O. Vasylenko, L. Zaprutko, A. Gzella, R. Lesyk. Eur. J. Med. Chem. 44 (2009) 1396–1404.
9. D. Kaminskyy, B. Zimenkovsky, R. Lesyk. Eur. J. Med. Chem.44 (2009) 3627–3636.
10. O. Ates, H. Altıntas, G. Otuk, Arzneim. Forsch. Drug Res. 50 (2000) 569–575.
11. A. Kocabalkanl, O. Ates, G. Otuk, Arch. Pharm. Med. Chem. 334 (2001) 35–39.
12. S.G. Kucukguzel, E.E. Oruc, S. Rollas, F. Sahin, A. Ozbek, Eur. J. Med. Chem. 3 (2002) 197–206.
13. V. S. Palekar, A. J. Damle, S.R. Shukla, Eur. J. Med. Chem.44 (2009) 5112–5116.

14. N. Cesur, Z. Cesur, N. Ergenc, M. Uzun, M. Kiraz, O. Kasımoglu, D. Kaya, Arch. Pharm. Weinheim.327 (1994) 271–273.
15. N. Karali, E. Ilhan, A. Gursoy, M. Kiraz, Farmaco.53 (1998) 346–349.
16. H. T. Y. Fahmy, Boll. Chim. Farmaco. 140 (2001) 422–427.
17. M. L. Barreca, A. Chimirri, L. D. Luca, A. M. Monforte, P. Monforte, A. Rao, M. Zappala, J.Balzarini, E. De Clercq, C. Pannecouque, M. Witvrouw, Bioorg.Med. Chem. Lett.11(2001)1793–1796.
18. A. Rao, A. Carbone, A. Chimirri, E. D. Clercq, A. M. Monforte, P. Monforte, C. Pannecouque, M. Zappala, Farmaco.57 (2002) 747–751.
19. Rao, A. Carbone, A. Chimirri, E.D. Clercq, A.M. Monforte, P. Monforte, C. Pannecouque, M. Zappala, Farmaco.58 (2003) 115–120.
20. M. Chayah, M. D. Carriûn, M. A. Gallo, R. Jimnez, J. Duarte, M. E. Camacho. ChemMedChem. 10(2015)874–882.
21. R. Pingaew, P. Tongraung, A. Worachartcheewan, C. Nantasenamat, S. Prachayasittikul, S. Ruchirawat, V. Prachayasittikul. Med Chem Res. 22 (2013) 4016–4029.
22. M. Mushtaque, F. Avecilla, A. Azam. Eur. J. Med. Chem. 55 (2012)439–448.
23. M. Mushtaque, M. Jahan, M. Ali, M. S. Khan, M. Shahid Khan, P. Sahay, A. Kesarwani, Journal of Molecular Structure. 1122 (2016) 164–174.
24. M. Mushtaque, F. Avecilla, Z. B. Hafeez, M. Jahan, M. S. Khan, M. M. A. Rizvi, M. Shahid Khan, A. Srivastava, A. Mallik, S. Verma, Journal of Molecular Structure 1127 (2017) 99–113
25. A. D. Becke. Phys. Rev. A38. 6(1988) 3098–3100.
26. C. Lee, W. Yang, R. G. Parr 1988. Phys. Rev.B37 (1988) 785–789.
27. M.J. Frisch, et al., Gaussian09, Revision A.02, Gaussian, Inc., Wallingford CT, 2009.
28. Gaussian 03. Revision C.02.Wallingford CT: Gaussian Inc.; 2004.
29. S. Miertus, E. Scrocco, J.Tomasi, J.Chem. Phys. 55(1981)117–129.
30. K. Gholivand, C.O. Della V_edova, M.F. Erben, F. Mojahed, A.M. Alizadehgan, J. Mol. Struct. 840 (2007) 66–71.
31. D. Glossman-Mitnik, A. M_arquez-Lucero, J. Mol. Struct. Theochem 548 (2001) 153-163.
32. M. F. Erben, C.O. Della Vedova, R. Boese, H. Willner, C. Leibold, H. Oberhammer, Inorg. Chem. 42 (2003) 7297–7303.

33. L. J. S. Knutsen, C. J. Hobbs, C. G. Earnshaw, A. Fiumana, J. Gilbert, S. L. Mellor, F. Radford, N. J. Smith, P. J.Birch, J. R. Burley, S. D. C. Ward, I. F. James, Bioorg. Med. Chem. Lett. 17 (2007) 662–667.
34. Jamróz, H. Michał. SpectrochimicaActa Part A: Molecular and Biomolecular Spectroscopy. 114 (2013) 220–230.
35. M. H. Jamro´z, J. Cz. Dobrowolski, R. Brzozowski. Journal of molecular structure. 787 (2006) 172–183.
36. C. T. Zeyrek, S. B. Koçak, H. Ünver, S. Pektas, N. S. Basterzi, O. Çelik . Journal of Molecular Structure 1100 (2015) 570–581.
37. T. A. de Toledo, L.E. da Silva, A. M. R. Teixeira , P.T.C. Freire, P. S. Pizani. Journal of Molecular Structure. 1091 (2015) 37–42.
38. A. A. Prasad, K. Muthu, M. Rajasekar, V. Meenatchi, S. P.Meenakshisundaram. SpectrochimicaActa Part A: Molecular and Biomolecular Spectroscopy. 135 (2015) 46–4.
39. A. Saeed, A. Khurshid, M. Bolte, A. C. Fantoni, M. F. Erben. SpectrochimicaActa Part A: Molecular and Biomolecular Spectroscopy. 143 (2015) 59–66.
40. J. P. Foster, F. Weinhold, J. Am. Chem. Soc. 102 (1980) 7211–7218.
41. F.Weinhold, C. R. Landis. Cambridge University press 2005. (www.cambridge.org/9780521831284).
42. S. T. Vallejos, M. F. Erben, O. E. Piro, E. E. Castellano, C. O. Della Védova. Polyhedron. 28 (2009) 937–946.
43. M. F. Erben, R. Boese, C. O. Della Ve´dova, H. Oberhammer, H. Willner. Journal of organic chemistry. 71 (2006) 616–622.
44. A. Saeed, A. Khurshid, J. P. Jasinski, C. G. Pozzi, A. C. Fantoni, M. F. Erben. Chemical Physics. 431 (2014) 39–46.
45. Diego M. Gil, M.E. Defonsi Lestard, O. Estevez-Hernandez, J. Duque , E. Reguera. Spectrochimica Acta Part A: Molecular and Biomolecular Spectroscopy 145 (2015) 553–562.
46. E. Kavitha, N. Sundaraganesan, S. Sebastian, M. Kurt. Spectrochim. Acta A. 77(2010)612-619.
47. R. J. Parr, L.V. Szentpaly, S. Liu, J. Am. Chem. Soc.121 (1999)1922-1924.

48. A. Saeed, M. I. Arshad, M. Bolte, A. C. Fantoni, Z. Y. Delgado Espinoza, M. F. Erbend. SpectrochimicaActa Part A: Molecular and Biomolecular Spectroscopy.157 (2016) 138–145.
49. V.V. Aswathy, Y. S. Mary, P. J. Jojo, C. Y. Panicker, A. Bielenica, S. Armakovi, S. J. Armakovi, P. Brz, ozka, S. Krukowski, C. V. Alsenoy. J. of Mol. Struc. 1134 (2017) 668-680.
50. J. A. War, K. Jalaja, Y. S. Mary, C. Y. Panicker, S. Armakovi, S. J. Armakovi, S. K. Srivastava, C. V. Alsenoy. J. Mol. Struc.1129 (2017) 72-85.
51. K. N. Houk, S. Menzer, S. P. Newton, F. M. Raymo, J. F. Stoddart, D. J. Williams, J. Am. Chem. Soc.121 (1999) 1479–1487.
52. J. J. Novoa, F. Mota, Chem. Phys. Lett.318 (2000) 345–354.
53. M. N. Patel, P.A. Parmar, D.S. Gandhi, A.P. PatidarSpectrochimicaActa Part A: Molecular and Biomolecular Spectroscopy. 97 (2012) 54–59.
54. Eric, Long, K. Jacqueline. Acc. Barton. Chem. Res. 23 (1990) 271–273.
55. T. A. Koopmans, Physica.1 (1934) 104–113.
56. S. M. Thom, R.W. Horobin, E. Seidler, M. R. Barer. Appl. Bacteriol. 7 (1993) 433–443.
57. B. Kitchen, H. Decornez, J. R. FurrBajorath. J. Nat. Rev. Drug Discov. 3 (2004) 935–949.
58. S. M. Thom, R.W. Horobin, E. Seidler, M. R. Barer. Appl. Bacteriol.74 (1993) 433–443.
59. S. R. Kim, M. J. Park, M. K. Lee, S. H. Sung, E. J. Park , FreeRadic. Biol. Med. 32(2002) 596–604.
60. S. H. Kim, J. H. Zo, M.A. Kim, K.K. Hwang, I. H. Chae. Nutr. Res. 23 (2003) 1671–1683.
61. H.Y. Lina, S.H. Juan, S.C. Shen, F.L. Hsu, Y.C. Chen. Biochem. Pharmacol. 66 (2003) 1821–1832.
62. B. Kitchen, H. Decornez, J. R. FurrBajorath, J.; *Nat. Rev. Drug Discov*. 3 (2004) 935–949.
63. G.M. Morris, D.S. Goodsell, D.S.Halliday, R. Huey, WE. Hart R. Belew A.J. Olson J. Comp. Chem.19(1998) 1639–1662.
64. R. Huey, G.M. Morris, A. J. Olson, D. S. Goodsell, J. Comp. Chem. 28 (2007) 1145–1152.
65. O. Trott, A. Olson, *J. Comp. Chem*. 31(2010) 455–461.
66. G. M. Sheldrick, *SADABS*, version 2.10, University of Göttingen, Germany, (2004).
67. *SHELX*, G. M. Sheldrick, ActaCrystallogr., Sect. A 64 (2008) 112–122.

68. M. K. Gupta, T.V. Neelakantan, M. Sanghamitra, R.K. Tyagi, A. Dinda, S. Mualik, C. K. Mukhopadhyay, Goswami. S.K.; *Antioxi. Redox Signal*. 8(2006) 1081–1093.
69. S.J. Mehdi, A. Ahmad, M. Irshad, Cytotoxic effect of Carvacrol on human cervical cancer cells. BM, 3 (2011) 307–12.
70. M. Irshad, S. J. Mehdi, A. A. Al-Fatlawi, Phytochemical Composition of Cassia fistula Fruit Extracts and its Anticancer Activity Against Human Cancer Cell Lines. J Biologically Active Prod Nat. 4(2014)158–70.
71. A. Wolfe, G. H. Shimer, Jr. Meehan, T. Biochemistry. 26 (1987)6392–6396.
72. M. F.; Sanner, *J. Mol. Graph Model*. 17(1999**)**57–61.
73. M. Morris, G. S. Goodsell, R. S. Halliday, R. Huey, W. E. Hart, R. Belew, A. J Olson. J. Comput.Chem.19(1998**)**1639–1662.
74. W. W Lai, J. S Yang, K. C Lai, C. L Kuo, C. K Hsu, C. K Wang. Rhein induced apoptosis through the endoplasmic reticulum stress, caspase-and mitochondria-dependent pathways in SCC-4 human tongue squamous cancer cells. *In Vivo*. 23 (2009) 309–316.

Caption illustrations

Caption figures

Caption tables

Caption figures

Fig.1(a-b): Thiourea derivatives displaying nNOS activity(a) and inducible activity against iNOS activity

Fig.2(a-b):Thiourea derivatives showing promising cytotoxicity against HepG2 and MOLT-3 cell lines.

Fig.(3): X-ray single crystal structure of 1-(4-methoxyphenyl)-3-(pyridine-2-ylmethyl)thiourea

Fig. (4): Part of the crystal packing in the compound 1-(4-methoxyphenyl)-3-(pyridine-2-ylmethyl)thiourea. Hydrogen bonds between nitrogen atoms of secondary amines with nitrogen atoms of pyridine groups and sulphur atoms are presented in dark dashes lines

Fig. 5(a-c):Optimized structure of 3-(4-methoxyphenyl)-1-(pyridine-2-ylmethyl) thiourea

Fig. 6(a-b): Experimental and (b)theorical IR-spectra of 3-(4-methoxyphenyl)-1-(pyridin-2-

ylmethyl)thiourea

Fig.7: (a-b) Experimental & (b) theoretical UV-visible spectra of 3-(4-methoxyphenyl)-1-(pyridin-2-ylmethyl)thiourea

Fig.(8):Frontiermolecular orbitals of 3-(4-methoxyphenyl)-1-(pyridine-2- ylmethyl)thiourea

Fig.(9): Energy gap between HOMO and LUMO molecular orbitals

Fig. 10(a): DNA binding spectra of 3-(4-methoxyphenyl)-1-(pyridine-2-yl methyl)thiourea

Fig.10 (b): DNA binding spectra of compound in the presence of increasing amount of Ct-DNA. Inset: plots of [DNA]/(εa− εf) (M2 cm^{-1}) versus [DNA] for the titration of CT DNA with compound. Experimental data points; full lines, linear fitting of the data (Compound) 2.0 x 10^{-4} M, [DNA] 0.3-1.5 x 10^{-5} M

Fig.11(a-c): Cell cycles phase distribution against HepG2 cells at 40µM & 80µM.

Fig.11(d-f): Cell cycles phase distribution against Siha cells at 40µM & 80µM

Fig.12(a-c): Cytotoxic effects of 3-(4-methoxyphenyl)-1-(pyridine-2-yl methyl)thiourea against (a)Siha(b) HepG2 (c) HEK-293 Cell

Fig. (13):3D-image of interactions of between DNA(PDBID: 1BNA) and ligand3-(4-

Caption Tables

Table(1): Frontier molecular orbital descriptors of 3-(4-methoxyphenyl)-1-(pyridin-2-ylmethyl)thiourea at B3LYP/6-311++G(d,p) level

Table(2): Crystal Data and Structure Refinement for the compound 1-(4-methoxyphenyl)-3-(pyridine-3-ylmethyl)thiourea

Caption Figures

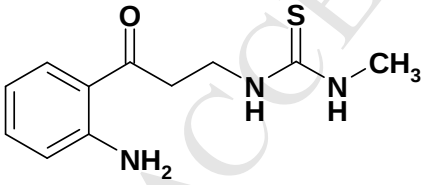

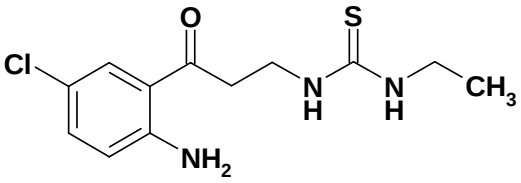

1(a)=(IC_{50} = 0.18 µM against nNOS) **(1b)=(IC_{50} = 0.59 µM against iNOS)**

Fig1(a-b): Thiourea derivatives displaying nNOS activity(a) and inducible activity against NOS activity.

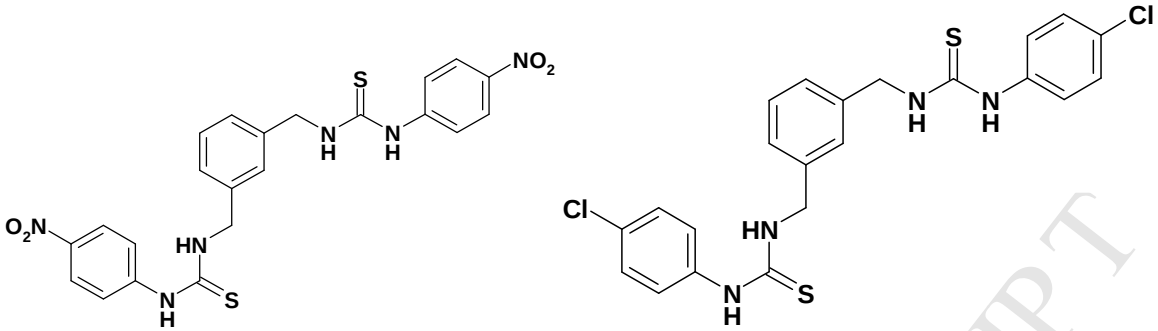

2(a) **2 (b)**

Fig.2(a-b):Thiourea derivatives showing promising cytotoxicity against HepG2 and MOLT-3 cell lines.

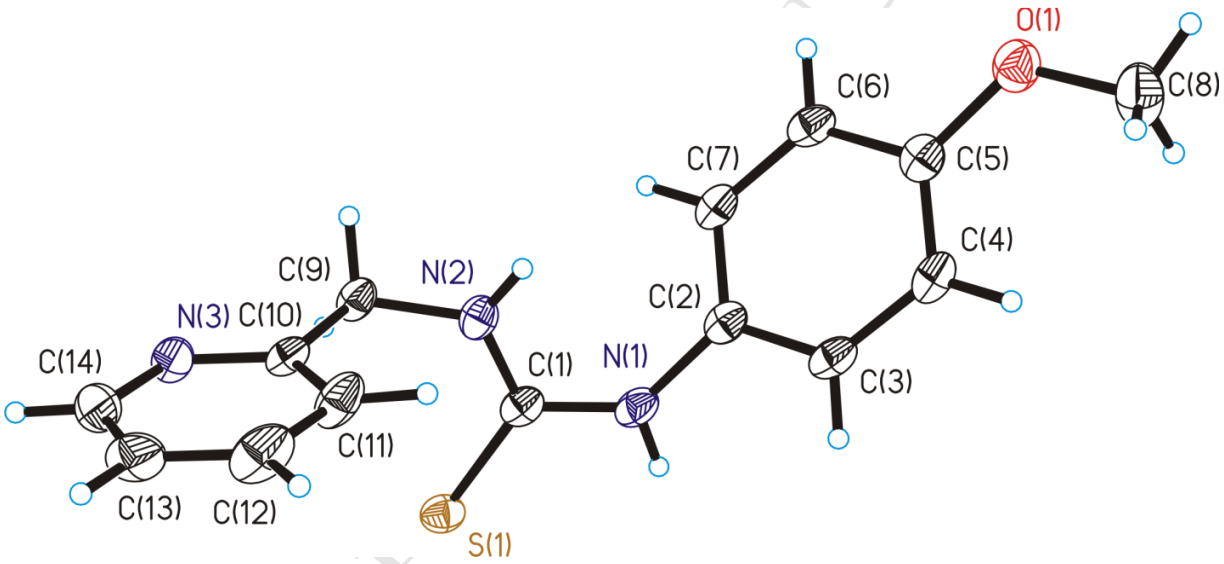

Fig. (3): X-ray single crystal structure of 1-(4-methoxyphenyl)-3-(pyridine-2-ylmethyl)thiourea

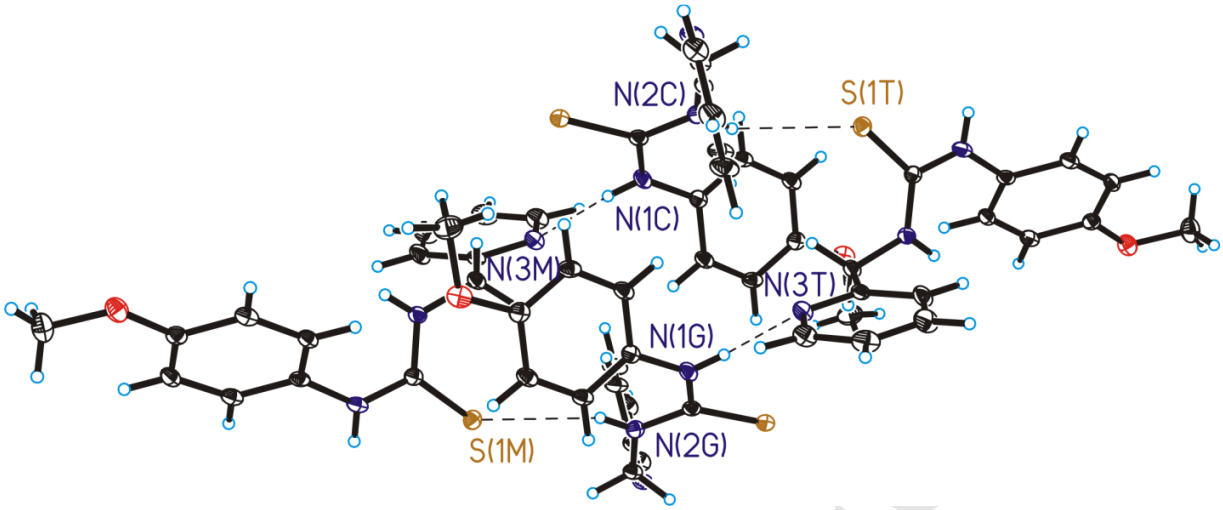

Fig. (4): Part of the crystal packing in the compound 1-(4-methoxyphenyl)-3-(pyridine-2-ylmethyl)thiourea (3). Hydrogen bonds between nitrogen atoms of secondary amines with nitrogen atoms of pyridine groups and sulphur atoms are presented in dark dashes lines

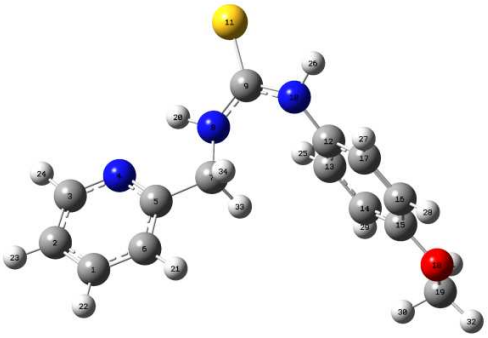

Fig. 5(a)

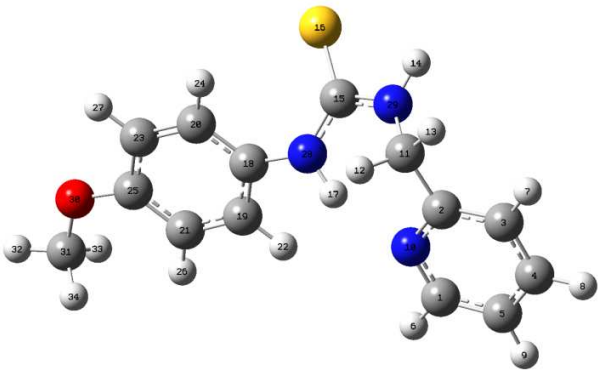

Fig.5(b)

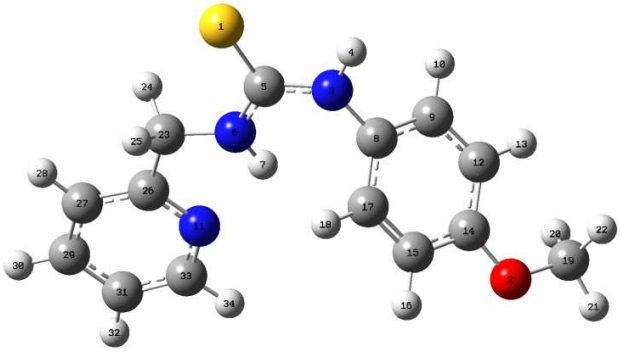

Fig.5(c)

Fig.5 :(a-c):Optimized structure of 3-(4-methoxyphenyl)-1-(pyridine-2-ylmethyl) thiourea

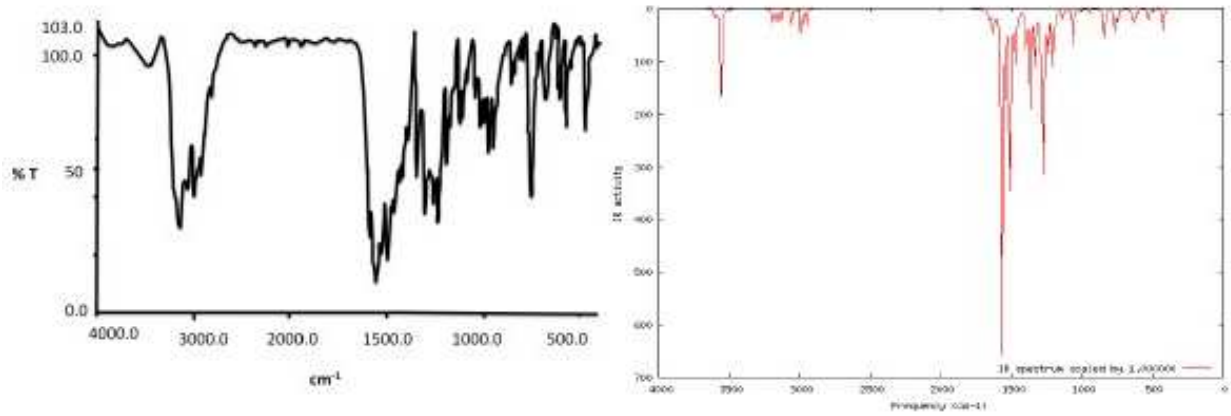

6(a) **6(b)**

Fig. 6(a-b): Experimental and (b) theoretical IR-spectra of 3-(4-methoxyphenyl)-1-(pyridin-2-ylmethyl)thiourea

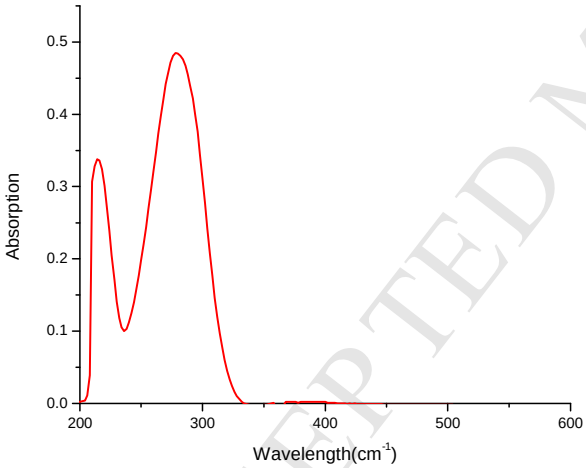

7(a)

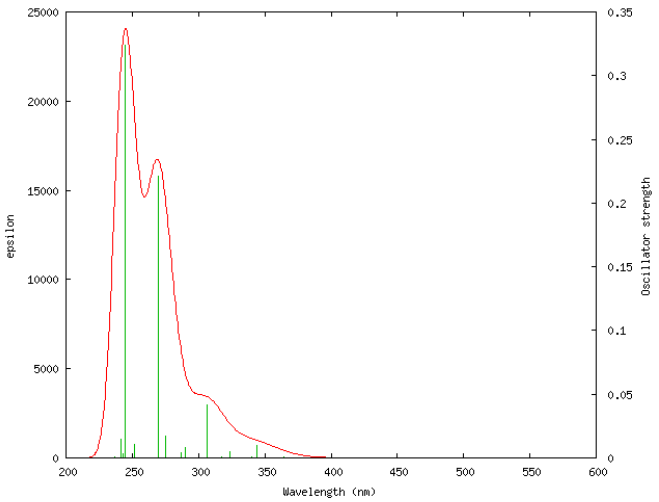

7(b)

Fig. 7: (a) Experimental & (b) theoretical UV-visible spectra of 3-(4-methoxyphenyl)-1-(pyridin-2-ylmethyl)thiourea

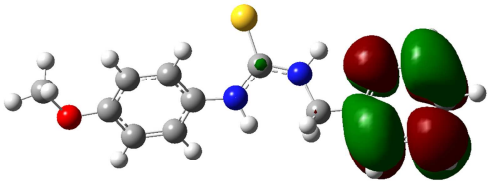

LUMO

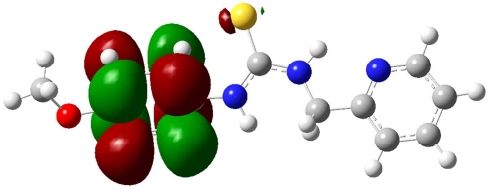

LUMO+1

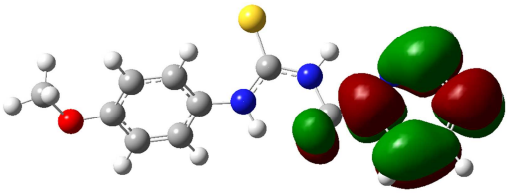

LUMO+2

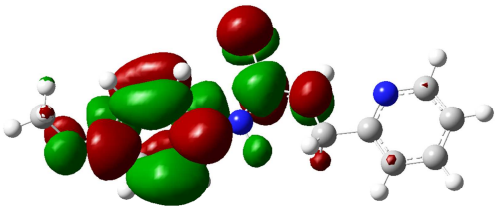

LUMO+3

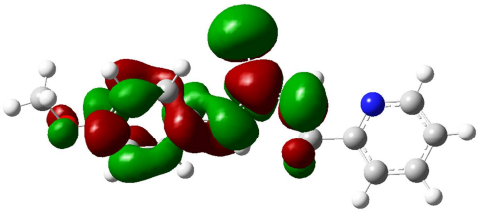

LUMO+4

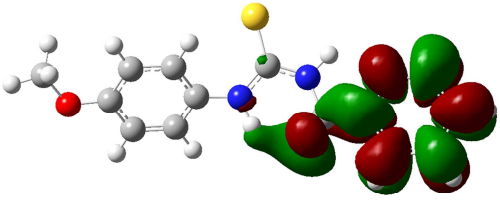

LUMO+5

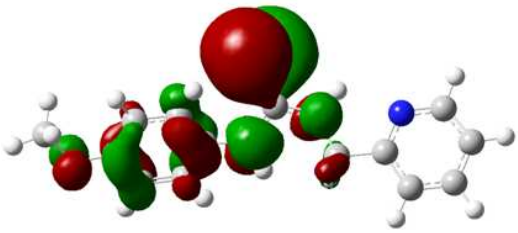

HOMO

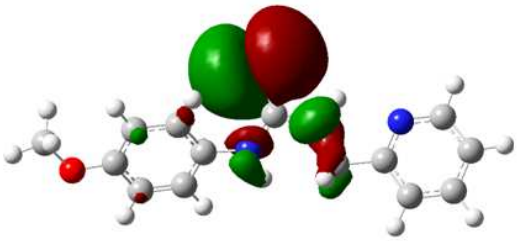

HOMO-1

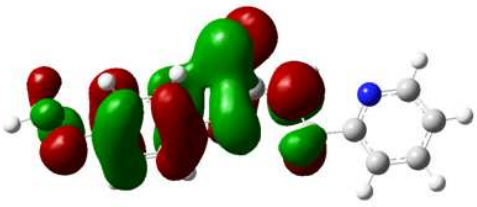

HOMO-2

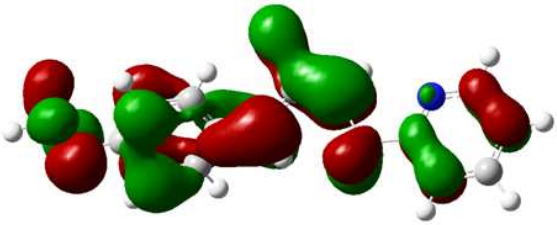

HOMO-3

Fig.(8): Molecular orbitals of 3-(4-methoxyphenyl)-1-(pyridine-2-ylmethyl)thiourea.

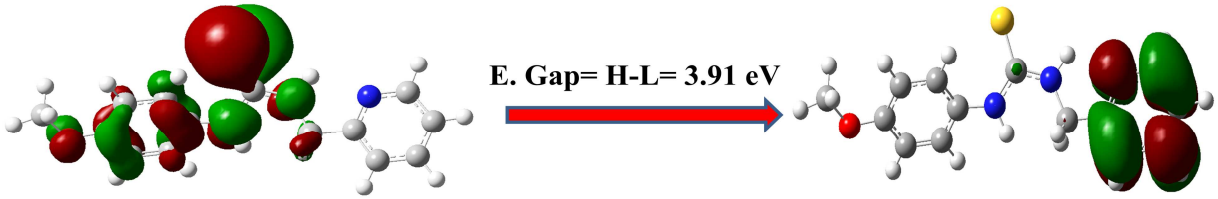

E_{HOMO} = -5.31 eV E_{LUMO} = -1.40 eV

Fig.(9): Energy gap between HOMO and LUMO molecular orbitals

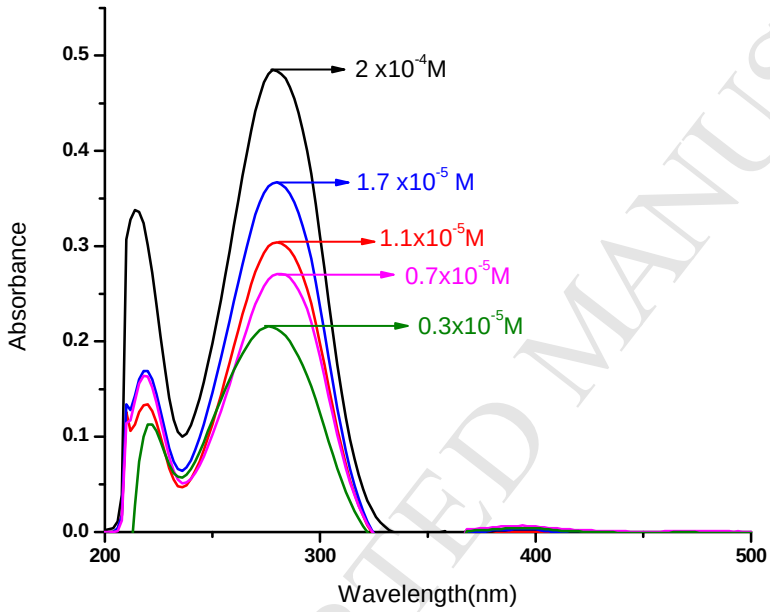

Fig.10(a): DNA binding spectra of 3-(4-methoxyphenyl)-1-(pyridine-2-yl methyl)thiourea

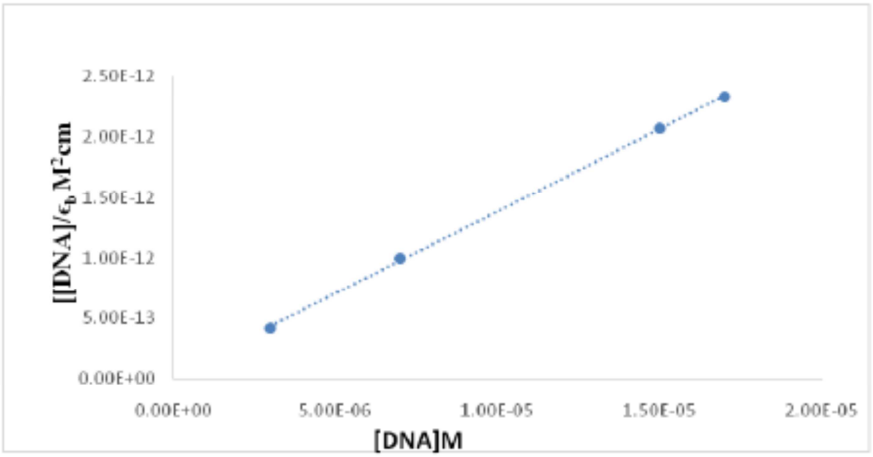

Fig.10(b): DNA binding spectra of compound in the presence of increasing amount of Ct-DNA. Inset: plots of [DNA]/(εa− εf) (M^2 cm^{-1}) versus [DNA] for the titration of Ct-DNA with compound. Experimental data points; full lines, linear fitting of the data (Compound) 2.0 x 10^{-4} M, [DNA] 0.3-1.5 x 10^{-5} M

Effect of compound (3) on cell cycle in HepG2

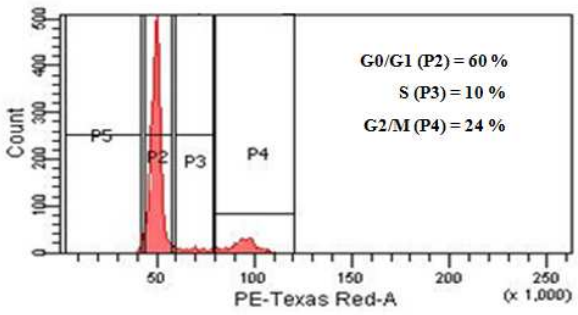

Fig.(a) Control

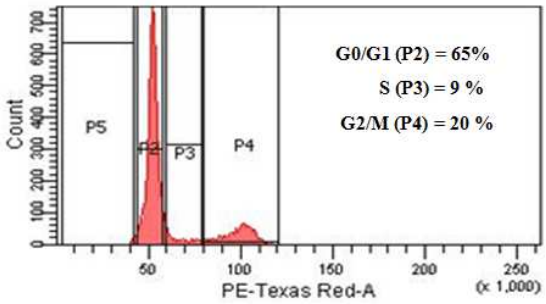

Fig. (b) Compound (3) 40 µM

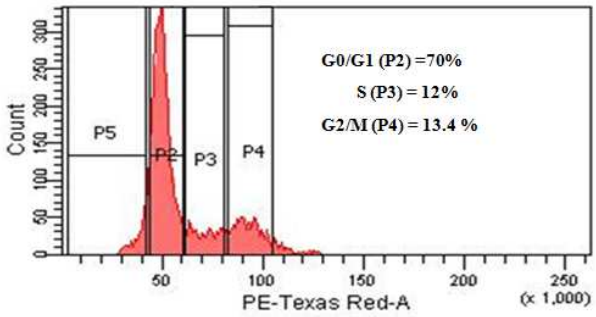

Fig.(c) Compound (3)80 µM

Fig. 11(a-c): Cell cycles phase distribution against HepG2 cells at 40µM & 80µM.

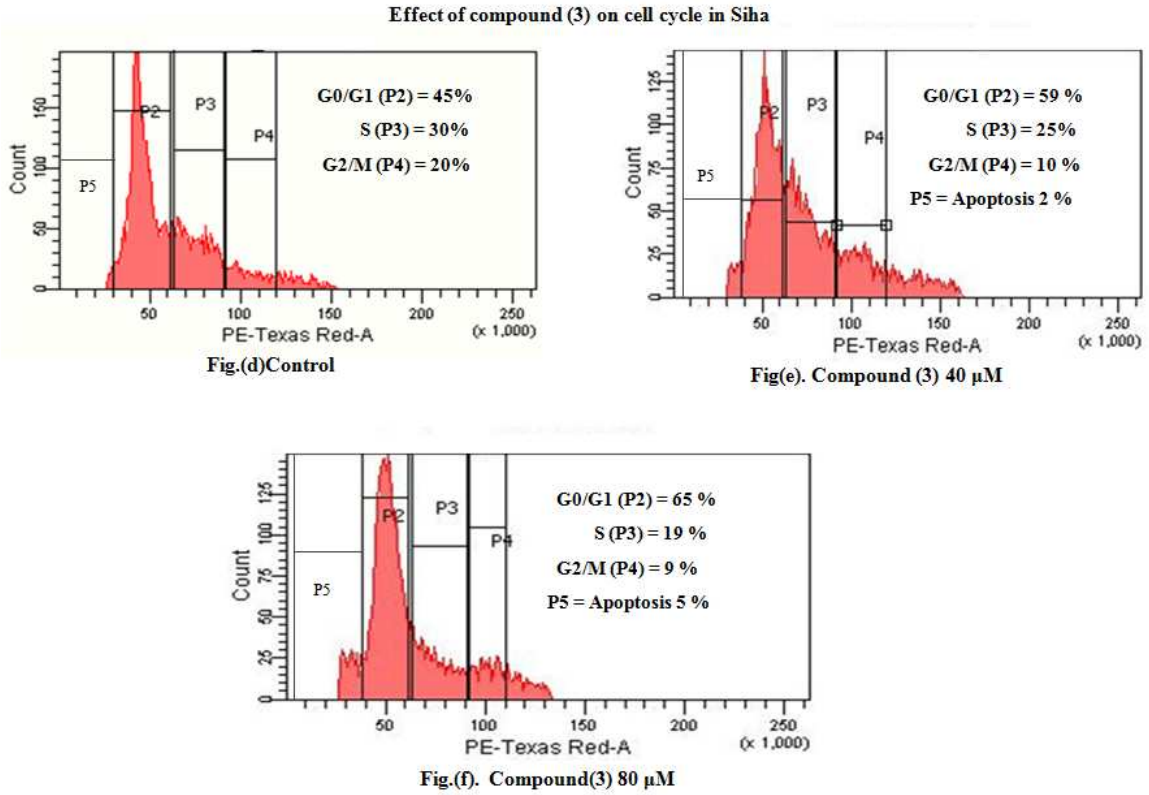

Fig.11(d-f): Cell cycles phase distribution against Siha cells at 40µM & 80µM

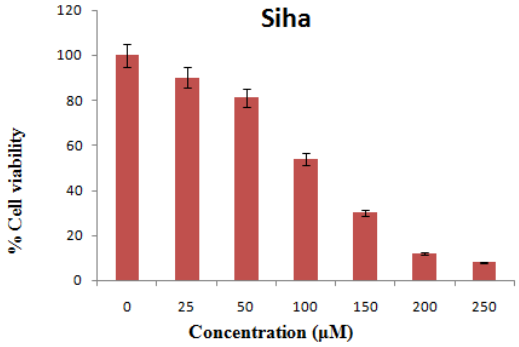

Fig. (a)

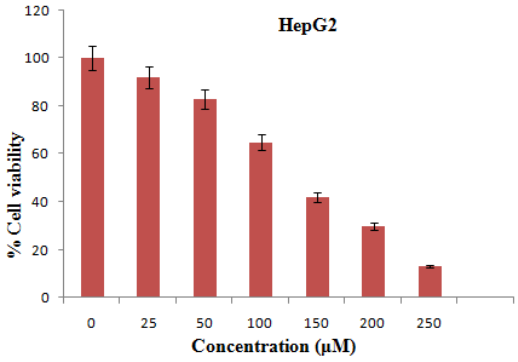

Fig. (b)

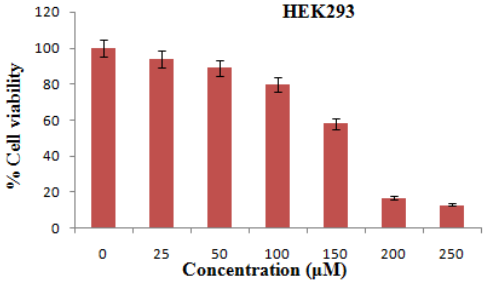

Fig. (c)

Fig.12(a-c): Cytotoxic effects of 3-(4-methoxyphenyl)-1-(pyridine-2-yl methyl)thiourea against (a)Siha(b) HepG2 (c) HEK-293 Cell

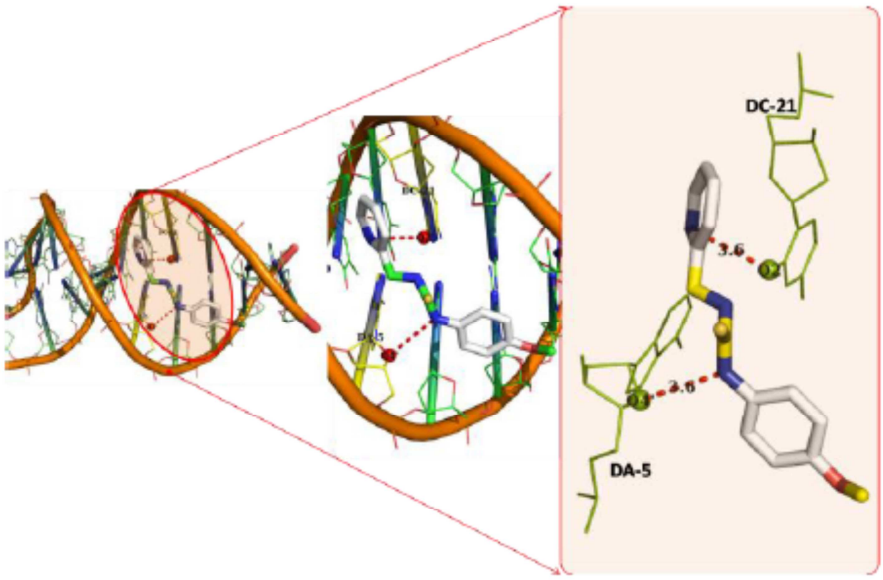

Fig.(13):3D image of interactions of between DNA(PDBID: 1BNA) and ligand3-(4-methoxyphenyl)-1-(pyridine-2-yl methyl)thiourea

Table(1): Frontier molecular orbital descriptors of 3-(4-methoxyphenyl)-1-(pyridin-2-ylmethyl)thiourea at B3LYP/6-311++G(d,p) level

Molecular Parameters	Mathematical expression	B3LYP/6-311++G(d,p)
E_{HOMO}(eV)	-	-5.31
E_{LUMO}(eV)	-	-1.40
E.Gap(H-L) (eV)	H-L	3.91
Ionization energy(I.E) = - E_{HOMO}(eV)	I.E = - E_{HOMO}(eV)	5.31
Electron affinity(E.A) = - E_{LUMO}(eV)	E.A = - E_{LUMO}	-1.40
Electronegativity (χ) (eV)	$\chi = (I+A)/2$	3.35
Chemical potential(μ) (eV)	$\mu = -\chi$	-3.35
Chemical hardness (η) (eV)	$\eta = (I-A)/2$	1.95
Chemical softness(s)(eV^{-1})	$s = 1/2\ \eta$	0.26
Global electrophilicity Index (ω) (eV)	$\omega = \mu^2/2\eta$	2.88

Table(2):Crystal Data and Structure Refinement for the compound 1-(4-methoxyphenyl)-3-(pyridine-2-ylmethyl)thiourea (3)

Compound	**3**
Formula	$C_{14}\ H_{15}\ N_3\ O\ S$
Formula weight	273.35
T, *K*	100(2)
Wavelength, Å	0.71073
Crystal system	Monoclinic
Space group	$P2_1/c$
a/Å	9.8888(13)
b/Å	13.3522(18)
c/Å	11.0985(15)
β/º	111.325(2)
V/Å^3	1365.1(3)
Z	4
F_{000}	576
D_{calc}/g cm^{-3}	1.330
μ/mm^{-1}	0.233
θ/ (º)	2.21 to 29.50
R_{int}	0.0391
Crystal size/ mm^3	0.49 x 0.42 x 0.39
Goodness-of-fit on F^2	1.028
$R_1[I>2\sigma(I)]$ [a]	0.0349
wR_2 (all data) [b]	0.0956
Largest differences peak and hole (eÅ^{-3})	0.371 and -0.231

[a] $R_1 = \Sigma \left|\left| F_o \right| - \left| F_c \right|\right| / \Sigma \left| F_o \right|$. [b] $wR_2 = \{\Sigma[w(\left|\left| F_o \right|^2 - \left| F_c \right|^2\right|)^2] / \Sigma[w(F_o^2)^2]\}^{1/2}$

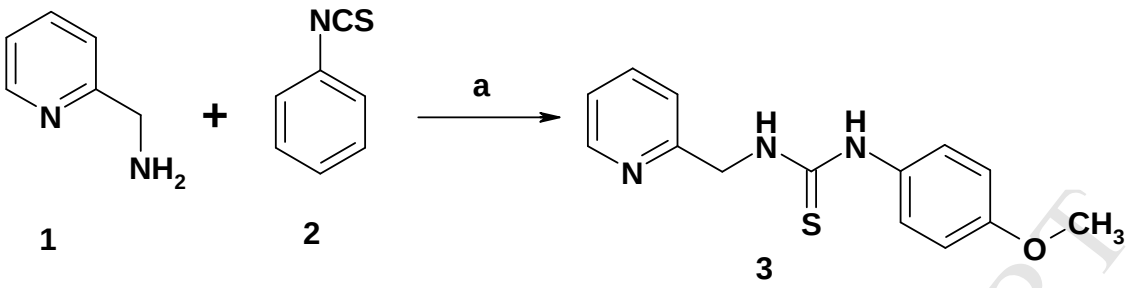

1 2 3

Scheme1: (a) Toluene, room temperature

- **compound(3) adopted *syn-anti*-conformation**
- **DNA-binding const K_b = 3.3 x 10^6 $Lmol^{-1}$**
- **Docking energy= -6.2 Kcal/mol**
- **IC_{50} values against HeG2,Siha & HEK-293 = 140 μM, 119.67& μM148.87 μM**